Journal of Korean Society of
Coastal and Ocean Engineers
Vol. 15, No. 4, pp. 224~231, December 2003

# Wave Screening Performance Using Floating and Submerged Breakwaters
# 부유식방파제와 잠제를 이용한 파랑 차단 성능 연구

Won Chul Cho* and Jin Won Lee*
조원철* · 이진원*

**Abstract** □ In this study, the hybrid breakwater system - a breakwater system combining the floating breakwater with the submerged breakwater - is used to improve the wave screening performance that may not be achieved by using the floating breakwater or the submerged breakwater, separately. Two-dimensional finite element method is used for numerical analysis and the wave reflection ratio and the wave transmission ratio are analyzed for the proposed case. In case of using the hybrid breakwater system, wave screening performance is more effective than in case of using the floating breakwater or the submerged breakwater, separately. It also shows an effective wave screening on the long wave period and an advanced wave screening performance with low height of the submerged breakwater.

**Keywords :** hybrid breakwater system, floating breakwater, submerged breakwater, finite element method, wave reflection coefficient, wave transmission coefficient

**要　旨 :** 본 논문에서는 부유식 방파제와 잠제의 단점을 보완하고 장점을 활용하기 위하여 부유식방파제와 잠제를 혼합한 혼합형 방파제에 의한 파랑 차단 성능을 2차원 유한요소법에 의해 검토하고 있다. 혼합형 방파제의 경우 부유식 방파제 또는 잠제를 단독으로 사용하였을 때 보다 우수한 파랑 차단 성능을 보였고, 단파 및 비교적 장파에서도 우수한 파랑 차단 성능을 보여 파랑의 일부 주기에 국한되지 않고 넓은 주기 영역에서의 파랑 차단 성능이 우수함이 나타났다.

**핵심용어 :** 혼합형 방파제, 부유식 방파제, 잠제, 유한요소법, 반사계수, 전달계수

## 1. Introduction

In order to develop and utilize coastal zone efficiently, various kinds of breakwaters should be studied and developed. Although the existing rubble mound breakwater is excellent in wave screening performance, it has some economical and technical problems in construction and management in deep water. It also deteriorates sea water quality and causes sea water pollution behind breakwaters with blocking sea water circulation. From this point the floating breakwater or the submerged breakwater has been studied steadily and those breakwaters are considered the alternative breakwaters that are able to complement the weak point of the existing rubble mound breakwater (Frederiksen, 1971; Shashikala, Sundaravadivleu and Ganapathy, 1977; Hales, 1981; Kobayashi and Wurjanto, 1989; Van der meer and Deamen, 1994; Vathamony, 1995; Sannasiraj, Sundar and Sundaravadivelu, 1998).

In this study, the hybrid breakwater system - a breakwater system combining the floating breakwater with the submerged breakwater - is used to achieve the strong point and to complement the weak point of each breakwater. Two-dimensional finite element method is used for numerical analysis and the wave reflection ratio and the wave transmission ratio are analyzed.

## 2. Governing equation and boundary conditions

The fluid is assumed to be incompressible and inviscid, and the flow is irrotational. The fluid motion, therefore, can

*중앙대학교 공과대학 건설환경공학과(Corresponding author: Won Chul Cho, Department of Civil & Environmental Engineering, Chung-Ang University, 221 Huksuk-dong, Dongjak-gu, Seoul, 156-756, Korea. chowc@cau.ac.kr)

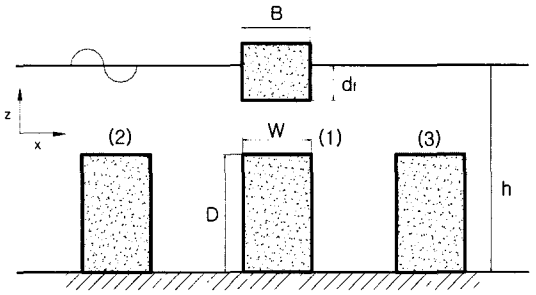


**Fig. 1.** Schematic definition of the breakwater for numerical model.

be expressed with the velocity potential, $\Phi$, which satisfies the Laplace equation.

$$\nabla^2\Phi(x,\ z;\ t)=\frac{\partial^2\Phi}{\partial x^2}+\frac{\partial^2\Phi}{\partial z^2}=0 \tag{1}$$

Boundary conditions at free surface ($S_f$), seabed ($S_d$), surface of the floating breakwater surface ($S_{b1}$) and surface of the submerged breakwater ($S_{b2}$) are as follows.

$$\frac{\partial\Phi}{\partial z}=\frac{\omega^2}{g}\Phi \ (\text{on } S_f),\quad \frac{\partial\Phi}{\partial n}=0 \ (\text{on } S_d)$$
$$\frac{\partial\Phi}{\partial n}=V_n \ (\text{on } S_{b1}),\quad \frac{\partial\Phi}{\partial n}=0 \ (\text{on } S_{b2}) \tag{2}$$

Where, $n$ is the outward unit normal from the boundary surface to the fluid domain, $V_n$ is the velocity of the floating breakwater surface in that direction and $g$ is the gravitational acceleration.

The velocity potential $\Phi$ is expressed as the sum of potential of each wave component.

$$\Phi=Re\left[\left(\phi_0+\phi_4+\sum_{j=1}^{3}\phi_j\xi_j\right)e^{-i\omega t}\right] \tag{3}$$

Where, $\phi_0$ is the velocity potential of the incident wave, $\phi_4$ is the velocity potential of the diffracted wave, $\phi_j$ is the velocity potential of the reflected wave in j-direction motion, $\xi_j$ is the complex amplitude in j-direction motion. j-direction motion consists in three components of sway ($\xi_1$), heave ($\xi_2$) and roll ($\xi_3$). The velocity potential by the diffracted wave at infinite boundary ($S_r$) must satisfy the following radiation condition.

$$\lim_{r\to\infty}\sqrt{r}\left(\frac{\partial\phi_j}{\partial r}-ik_0\phi_j\right)=0 \qquad \text{for } j=1,2,3,4 \tag{4}$$

Where, $k_0$ is the wave number, and $r=|x|$ and $i=\sqrt{-1}$.

The hydrodynamic pressure distribution, $p\ (x,\ z;\ t)$ on body surface or at arbitrary point in the fluid domain is given by the linearized Bernoulli equation as

$$p\ (x,\ z;\ t)=-\rho\frac{\partial\Phi}{\partial t}=Re\left[i\omega\rho\left(\phi_0+\phi_4+\sum_{j=1}^{3}\phi_j\xi_j\right)e^{-i\omega t}\right] \tag{5}$$

where, $\rho$ is the fluid density.

The wave force/moment components on the solid body can be obtained by integrating all of the hydrodynamic pressure at each point on the body. The wave forces in the horizontal and the vertical directions ($F_1$, $F_2$), and the moment about the origin ($F_3$) are described as follows.

$$F_j=-\int_{S_b}p(x,z,t)n_jS_b=Re\left[\left(F_j^e+\sum_{k=1}^{3}F_{jk}^r\right)e^{-i\omega t}\right]$$
$$\text{for } j=1,2,3 \tag{6}$$

Where, $F_j^e$'s represent the hydrodynamic exciting force components associated with $\phi_0+\phi_4$ and are identical to the wave force components for a fixed body. $F_{jk}^r$'s are the force components associated with the radiated wave potential, $\phi_k$ ($k$ = 1, 2, 3), and conveniently described in the conventional way by the added mass coefficients, $\mu_{ik}$, and the damping coefficients, $\lambda_{jk}$, such that

$$F_j^e=i\omega\rho\int_{S_b}(\phi_0+\phi_4)n_jdS_b \tag{7}$$

$$F_{jk}^r=i\omega\rho\int_{S_b}\phi_kn_jdS_b=-\omega^2\mu_{jk}-i\omega\lambda_{jk} \tag{8}$$

where,

$$\mu_{jk}=-\frac{1}{\omega^2}Re[F_{jk}^r] \tag{9}$$

$$\lambda_{jk}=-\frac{1}{\omega}Im[F_{jk}^r] \tag{10}$$

where, $\mu_{jk}$ and $\lambda_{jk}$ are real numbers, and $Im[]$ denotes the imaginary part of the argument.

By using the linear wave diffraction theory, the wave-structure interaction problems can be formulated as two boundary value problems, i.e., the diffraction problem of an incident wave, which interacts with a fixed body and is associated with $\phi_0$ and $\phi_4$, and the radiation problem of a freely floating body, which oscillates in otherwise still water and is associated with $\phi_j$ ($j$ = 1, 2, 3). In case of the submerged breakwater, only the diffraction problem can be

considered because the radiation problem does not occur. In case of the floating breakwater, however, the diffraction and radiation problems are considered because both problems occur coincidentally.

In this study, in order to analyze the boundary value problems efficiently, the entire fluid domain is divided into two regions; the inner finite element region surrounding the solid body and the outer infinite element region not surrounding the solid body. The inner region is analyzed by the finite element technique and the outer region is analyzed by the infinite element technique.

## 3. Comparison of the numerical results with the experimental results

### 3.1 Comparison of the numerical results of the submerged breakwater with the experimental results

The numerical results of the rectangular submerged breakwater are compared with the existing experimental results of the rectangular submerged breakwater performed by Losada and Patterson (1997). They performed the experiments with water depth, $h = 0.475$ m, height of the submerged breakwater, $D = 0.385$ m and width of the submerged breakwater, $W = 0.8$ m. Table 1 shows wave conditions using in the experiments of the submerged breakwater.

In the numerical analysis for the submerged breakwater, the same scale of water depth, height of the submerged breakwater and width of the submerged breakwater used in the experiments are used, and 100 wave conditions, $h/L$ 0.005~0.5 with the increment of 0.005 are used.

Fig. 2 and Fig. 3 show the comparison of the numerical results of the submerged breakwater with the experimental results performed by Losada and Patterson (1997). Fig. 2 shows the wave reflection ratio, and Fig. 3 shows the wave transmission ratio. The solid line and the circle represent the numerical result and the experimental result, respectively.

In Fig. 2, the wave reflection ratio of the numerical result

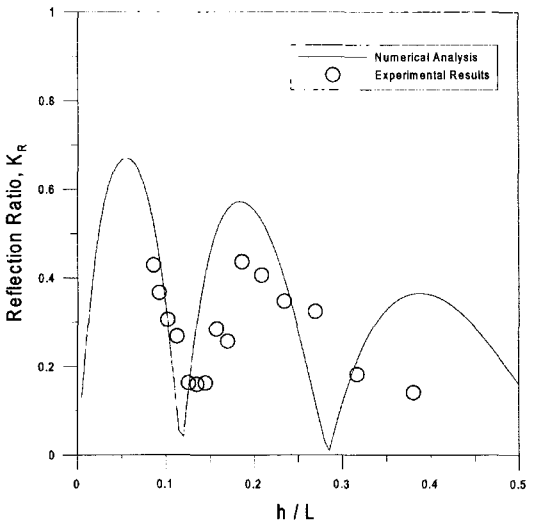


**Fig. 2.** Comparison of the wave reflection ratio of the numerical result of the submerged breakwater with that of the experimental result.

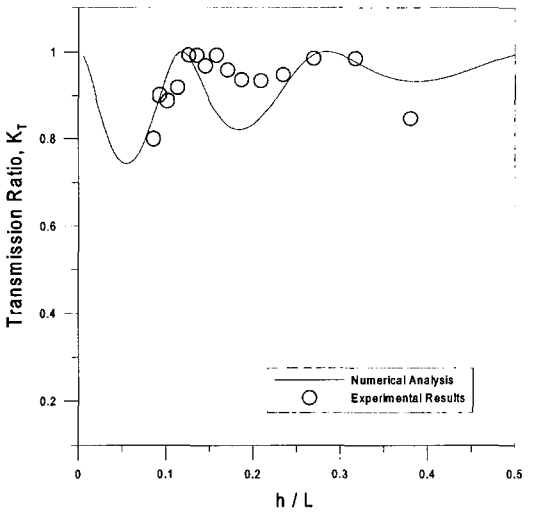


**Fig. 3.** Comparison of the wave transmission ratio of the numerical result of the submerged breakwater with that of the experimental result.

**Table 1.** Wave conditions using in the experiments of the submerged breakwater performed by Losada and Patterson (1997)

| T(sec) | 0.8 | 0.9 | 1.0 | 1.1 | 1.2 | 1.3 | 1.4 | 1.5 |
|---|---|---|---|---|---|---|---|---|
| H(cm) | 3.32 | 3.27 | 3.12 | 3.10 | 3.19 | 2.94 | 2.97 | 2.64 |
| h/L | 0.086 | 0.092 | 0.102 | 0.113 | 0.126 | 0.135 | 0.145 | 0.158 |
| T(sec) | 1.6 | 1.7 | 1.8 | 1.9 | 2.1 | 2.3 | 2.5 | |
| H(cm) | 3.08 | 2.91 | 2.66 | 2.26 | 2.55 | 2.77 | 1.96 | |
| h/L | 0.170 | 0.186 | 0.208 | 0.234 | 0.269 | 0.317 | 0.380 | |

is partly a little larger than that of the experimental result. The wave reflection ratio of the numerical result of the submerged breakwater, however, show a fairly good agreement with that of the experimental result.

In Fig. 3, like the result of the wave reflection ratio, the wave transmission ratio of the numerical result shows a little disagreement with that of the experimental result, at which the wave transmission ratio of the numerical result is partly a little smaller than that of the experimental result. However, the wave transmission ratio of the numerical result of the submerged breakwater also shows a fairly good agreement with that of the experimental result.

### 3.2 Comparison of the numerical results of the floating breakwater with the experimental results

The numerical results of the Pontoon-type floating breakwater are compared with the existing experimental results of the Pontoon-type floating breakwater performed in KORDI (Korea Ocean Research and Development Institute) (1992). KORDI performed the experiments with water depth, $h = 0.5$ m, length of the floating breakwater, $L_f = 0.98$ m, width of the floating breakwater, $B = 0.5$ m, height of the floating breakwater, $D_f = 0.2$ m, draft of the floating breakwater, $d_f = 0.1$ m, weight of the floating breakwater, $M = 49$ kg$_f$, moment of inertia, $M_i = 1.684$ kg · m and length of the mooring line, $L_m = 4$ m. Table 2. shows wave conditions using in the experiments of the floating breakwater

In the numerical analysis for the floating breakwater, the same scale of water depth, length of the floating breakwater, width of the floating breakwater, height of the floating breakwater, draft of the floating breakwater, etc. used in the experiments are used, and 100 wave conditions, $h/L =$ 0.005~0.5 with the increment of are used.

Fig. 4 and Fig. 5 show the comparison of the numerical results of the floating breakwater with the experimental results performed in KORDI (1992). Fig. 4 shows the wave reflection ratio, and Fig. 5 shows the wave transmission ratio. The solid line and the circle represent the numerical result and the experimental result, respectively.

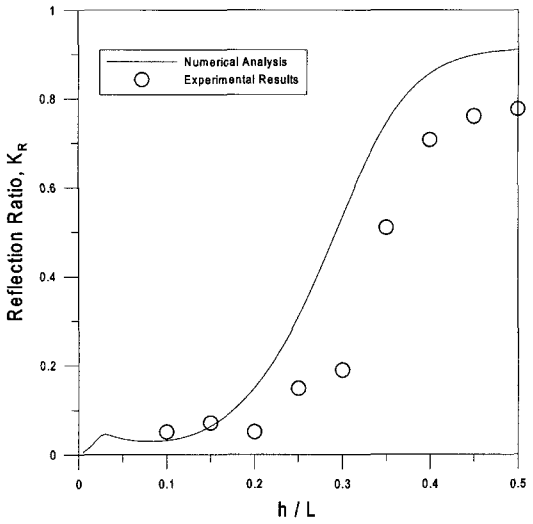


**Fig. 4.** Comparison of the wave reflection ratio of the numerical result of the floating breakwater with that of the experimental result.

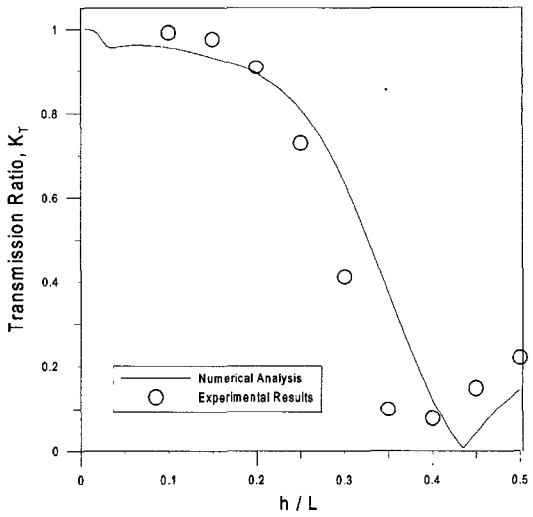


**Fig. 5.** Comparison of the wave transmission ratio of the numerical result of the floating breakwater with that of the experimental result.

In Fig. 4, the wave reflection ratio of the numerical result is partly a little larger than that of the experimental result. The wave reflection ratio of the numerical result of the floating breakwater, however, show a fairly good agree-

**Table 2.** Wave conditions using in the experiments of the floating breakwater performed by KORDI (1992)

| T(sec) | 0.8 | 0.85 | 0.9 | 0.97 | 1.06 | 1.18 | 1.37 | 1.70 | 2.40 |
|---|---|---|---|---|---|---|---|---|---|
| $H$(cm) | 3.0 | 4.0 | 4.0 | 5.0 | 6.0 | 8.0 | 8.0 | 8.0 | 8.0 |
| $h/L$ | 0.5 | 0.45 | 0.4 | 0.35 | 0.3 | 0.25 | 0.2 | 0.15 | 0.1 |

ment with that of the experimental result.

In Fig. 5, like the result of the wave reflection ratio, the wave transmission ratio of the numerical result shows a little disagreement with that of the experimental result, at which the wave transmission ratio of the numerical result is partly a little larger or a little smaller than that of the experimental result. However, the wave transmission ratio of the numerical result of the floating breakwater also shows a fairly good agreement with that of the experimental result.

## 4. Numerical results and discussions

In this study, the hybrid breakwater system - a breakwater system combining the floating breakwater with the submerged breakwater as shown in Fig. 1 - is used to analyze the characteristics of the wave reflection and transmission. The numerical analysis is performed in three cases; the case 1 - the submerged breakwater located just below the floating breakwater on the sea surface (Fig. 1(1)), the case 2 - the submerged breakwater located at one water depth offshore below the floating breakwater (Fig. 1(2)) and the case 3 - the submerged breakwater located at one water depth inshore below the floating breakwater on the sea surface (Fig. 1(3)).

The definition of the width ($B$) and the draft ($d_f$) of the floating breakwater, the width ($W$) and the height ($D$) of the submerged breakwater and the water depth ($h$) are shown in Fig. 1. $B/h = 1.0$ and $d_f = 0.2$ h are used for the floating breakwater. The submerged breakwater is considered as rectangular and impermeable, and $W/h = 1.0$ is used. 100 wave conditions are used in numerical analyses, varying the ratio of the water depth ($h$) and the incident wave length ($L$), $h/L$ from 0.005 to 0.5 with the increment of 0.005.

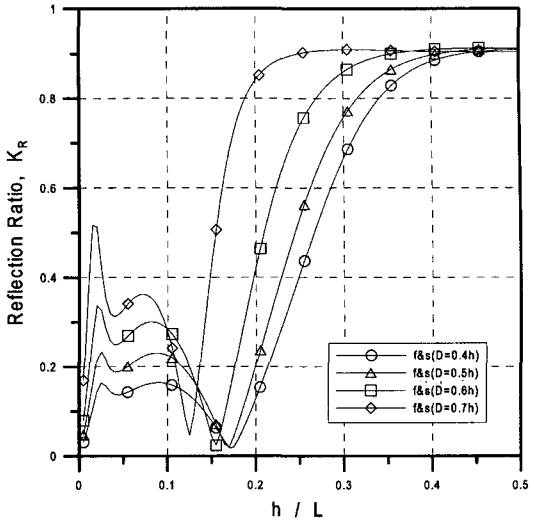


**Fig. 6.** The wave reflection ratio of the case 1.

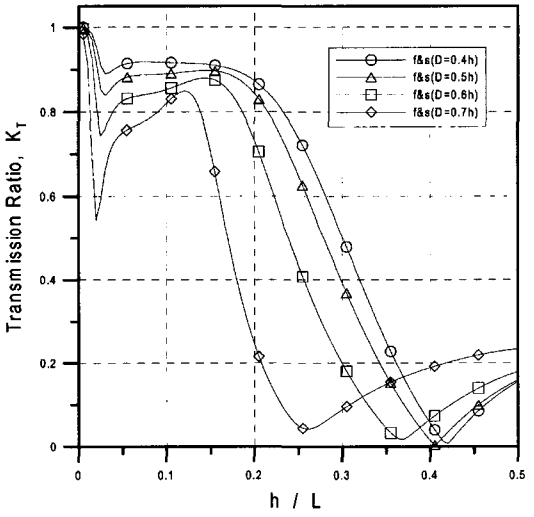


**Fig. 7.** The wave transmission ratio of the case 1.

### 4.1 The characteristics of the wave reflection and the wave transmission of the case 1 of the hybrid breakwater system

Fig. 6 and Fig. 7 show the wave reflection ratio, $K_R$ and the wave transmission ratio, $K_T$ of the case 1. The numerical analysis is carried out with the submerged breakwater height, $D = 0.4$ h, $D = 0.5$ h, $D = 0.6$ h and $D = 0.7$ h. In Fig. 6 and Fig. 7 '*f&s*' denotes $K_R$ and $K_T$ of the hybrid breakwater system of the case 1.

In the case 1 of the hybrid breakwater system, as shown in Fig. 6 and Fig. 7, as the submerged breakwater height is increased the range of the effective wave screening performance (large wave reflection ratio, $K_R$ and small transmission ratio, $K_T$) are extended from short wave period to relatively longer wave period. However, it does not show an effective wave screening performance with low height of the submerged breakwater.

### 4.2 Comparison of the wave reflection ratio and the wave transmission ratio of the case 1 of the hybrid breakwater system with the floating breakwater and the submerged breakwater

Fig. 8 and Fig. 9 show the comparison of $K_R$ and $K_T$ for $D = 0.7$ h of the case 1 with those of the floating breakwa-

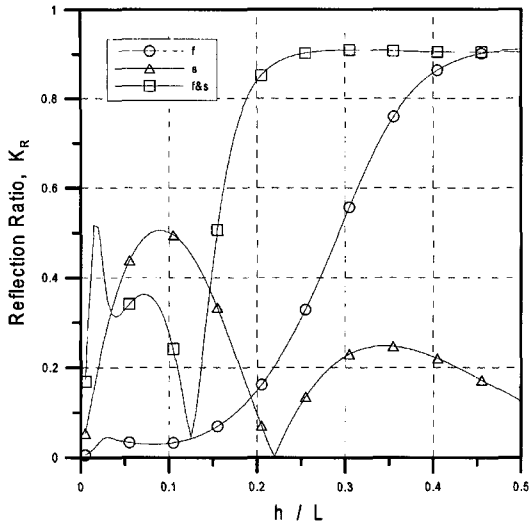


**Fig. 8.** Comparison of the wave reflection ratio of the case 1 with those of the floating breakwater and the submerged breakwater.

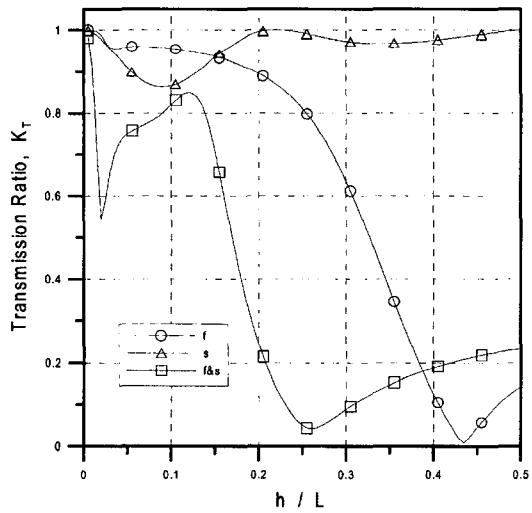


**Fig. 9.** Comparison of the wave transmission ratio of the case 1 with those of the floating breakwater and the submerged breakwater.

ter and the submerged breakwater. In Fig. 8 and Fig. 9 '*f*', '*s*' and '*f*&*s*' denotes $K_R$ and $K_T$ of the floating breakwater, the submerged breakwater and the case 1 of the hybrid breakwater system, respectively.

As shown in Fig. 8 and Fig. 9, the floating breakwater and the submerged breakwater show a good wave screening performance in short wave period and in long wave period, respectively. Comparing those breakwaters with the case 1 of the hybrid breakwater system, however, the effectiveness of wave screening performance of those breakwaters is much less than that of the case 1 except the wave reflection ratio in long wave for the submerged breakwater and the wave transmission ratio in short wave for the floating breakwater.

Fig. 8 shows the wave reflection ratio, $K_R$ of the case 1 of the hybrid breakwater system is larger than those of the floating breakwater and the submerged breakwater. In long wave period, at which $h/L$ smaller than 0.15, however, the submerged breakwater shows a better wave reflection than that of the case 1. In short wave period, at which $h/L$ greater than 0.45, the wave reflection ratio of the floating breakwater has the same value of the case 1. In Fig. 5, the case 1 of the hybrid breakwater system shows smaller wave transmission ratio, $K_T$ than that of the floating breakwater and the submerged breakwater except $h/L$ greater than about 0.38. Comparing the case 1 of the hybrid breakwater system with the floating breakwater and the submerged breakwaters, it appears that more effective wave screening performance can be obtained with the hybrid breakwater system.

### 4.3 Comparison of the wave reflection ratio and the wave transmission ratio of the case 1, case 2 and case 3 of the hybrid breakwater system

Fig. 10 and 11 show comparison of the wave reflection

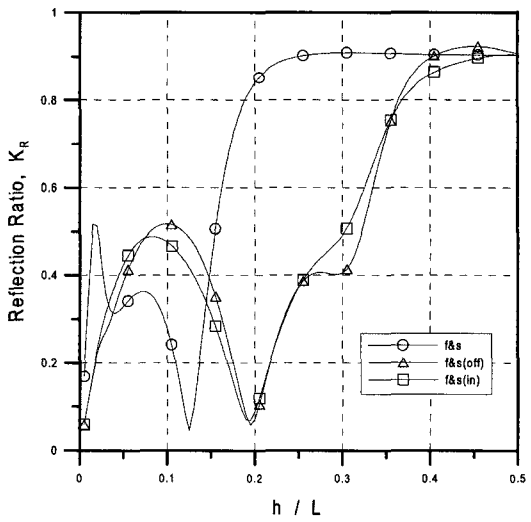


**Fig. 10.** Comparison of the wave reflection ratio of the case 1, case 2 and case 3 of the hybrid breakwater system.

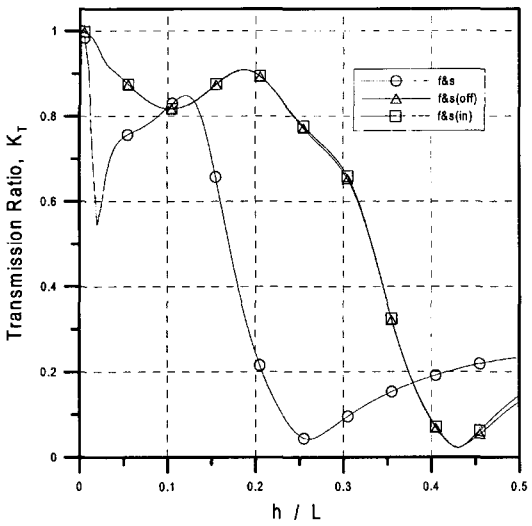


**Fig. 11.** Comparison of the wave transmission ratio of the case 1, case 2 and case 3 of the hybrid breakwater system.

ratio, $K_R$ and the wave transmission ratio, $K_T$ in the case 1, case 2 and case 3 for the submerged breakwater height, $D = 0.7$ h. In Fig. 6 and Fig. 7, '*f&s*' denotes $K_R$ and $K_T$ of the case 1, '*f&s*' denotes those of the case 2 and '*f&s(in)*' denotes those of the case 3.

As shown in Fig. 10 and Fig. 11, the case 2 and the case 3 of the hybrid breakwater system show almost same aspect in the wave reflection ratio and the wave transmission ratio. On the other hand, the case 1 shows much better wave screening performance with larger $K_R$ and smaller $K_T$ than that of the case 2 and the case 3. It is inferred, therefore, the location of the submerged breakwater offshore or inshore is not crucial, but the most effective wave screening performance appears in the hybrid breakwater system with the submerged breakwater located just below the floating breakwater.

## 5. Conclusion

Three cases of numerical analyses for the hybrid breakwater system is carried out to improve wave screening performance.

In case of the hybrid breakwater system, the wave reflection ratio is increased and the wave transmission ratio is decreased than those of the floating breakwater or the submerged breakwater, so that more effective wave screening performance can be obtained with the hybrid breakwater system. It is also found that in the hybrid breakwater system as the submerged breakwater height is increased the larger wave reflection ratio and the smaller wave transmission ratio are obtained, and the range of the effective wave screening performance are extended from short wave period to relatively longer wave period.

The case 2 and the case 3 of the hybrid breakwater system show almost same aspect in the wave reflection ratio and the wave transmission ratio, on the other hand, the case 1 shows much better wave screening performance than that of the case 2 and the case 3. It is found, therefore, the most effective wave screening appears in the hybrid breakwater system with the submerged breakwater located just below the floating breakwater.

## Acknowledgement

This work is supported by Chung-Ang University Research Grant. This support is greatly acknowledged.

## References

김도삼, 2000. 다열 잠제에 의한 파랑의 전달율과 반사율, 대한토목학회논문집, **20**(1-B), pp. 85-94.

양우석, 조원철, 박우선, 2001. 부유식 방파제의 파랑차단 성능제어. 한국해안 · 해양공학회지, **13**(3), pp. 230-236.

Frederiksen, H.D., 1971. Wave attenuation by fluid filled bags. Journal of the Waterway, *Harbors and coastal Engineering Division*, ASCE 97, pp. 73-90.

Hales, L.Z., 1981. *Floating breakwaters: State of the Art Literature Review.* Technical Report No. 81-1, Coastal Engineering Research Center, US Army Corps of Engineers, Fort Belvoir, VA.

Kobayashi, N. and Wurjanto, A., 1989. Wave transmission over submerged breakwaters. Journal of Waterway, *Port, Coastal and Ocean Engineering*, ASCE, **115**(5), pp. 662-680.

Korea Ocean Research and Development Institute, 1992. Development of improving quality in harbor(1)

Losada, I.J. and Patterson M.D. 1997. Harmonic generation past a submerged porous step. *Coastal Engineering*, **31**, pp. 281-304.

Sannasiraj, S.A. Sundar, V. and Sundaravadivelu. R., 1998. Mooring forces and motion responses of pontoon-type floating breakwaters. *Ocean Engineering*, **25**(1), pp. 27-48

Shashikala, A.P., Sundaravadivleu, P. and Ganapathy, C., 1977. Dynamics of a moored barge under regular and ramdom

waves. *Ocean Engineering*, **24**(5), pp 401-430.

Van der meer, J.W. and Deamen, F.R., 1994. Stability and wave transmission at low-crested rubble mound structures. Journal of Waterway, Port, *Coastal and Ocean Engineering*, ASCE, **120**(1), pp. 1-19.

Vathamony, P., 1995. Wave attenuation characteristics of a tethered float system. *Ocean Engineering*, 22, pp. 111-129.

Received August 18, 2003
Accepted November 3, 2003